Molecular Crystals and Liquid Crystals

Publication details, including instructions for authors and subscription information:
http://www.tandfonline.com/loi/gmcl20

Photoinduced Alignment and Multi-Processes of Refractive-Index Gratings in Pre-Irradiated Films of an Azobenzene-Containing Liquid-Crystalline Polymer

Haifeng Yu [a], Atsushi Shishido [a], Tomokazu Iyoda [a] & Tomiki Ikeda [a]

[a] Chemical Resources Laboratory, Tokyo Institute of Technology, Yokohama, Japan

Version of record first published: 22 Sep 2010

To cite this article: Haifeng Yu, Atsushi Shishido, Tomokazu Iyoda & Tomiki Ikeda (2007): Photoinduced Alignment and Multi-Processes of Refractive-Index Gratings in Pre-Irradiated Films of an Azobenzene-Containing Liquid-Crystalline Polymer, Molecular Crystals and Liquid Crystals, 470:1, 71-81

To link to this article: http://dx.doi.org/10.1080/15421400701492788

Mol. Cryst. Liq. Cryst., Vol. 470, pp. 71–81, 2007

ISSN: 1542-1406 print/1563-5287 online
DOI: 10.1080/15421400701492788

Taylor & Francis
Taylor & Francis Group

Photoinduced Alignment and Multi-Processes of Refractive-Index Gratings in Pre-Irradiated Films of an Azobenzene-Containing Liquid-Crystalline Polymer

Haifeng Yu
Atsushi Shishido
Tomokazu Iyoda
Tomiki Ikeda
Chemical Resources Laboratory, Tokyo Institute of Technology, Yokohama, Japan

After being pre-treated upon irradiation of unpolarized light at 366 nm, an azobenzene-containing liquid-crystalline polymer film was photoinduced alignment by one linearly polarized laser beam at 488 nm, leading to a large birefringence of 0.21. Then holographic gratings were recorded in the pre-irradiated polymer films by interference of two coherent laser beams. Little surface relief was obtained by the holographic recording process, indicating that a refractive-index grating paid most of contributions to the diffraction efficiency. Because the cooperative motion of the azobenzene mesogens were eliminated in the cis-azobenzene-rich isotropic film by the pre-irradiation, multi-processes of the refractive-index gratings were successfully achieved. The obtained grating structures were clearly shown in the polarizing optical microscopic pictures, which were also verified by their diffraction patterns. The azobenzene-containing liquid-crystalline polymer used in this study has potential application in high-density information storage.

Keywords: azobenzene-containing polymers; liquid-crystalline polymers; multi-processes of gratings; photochemical phase transition; refractive-index gratings

INTRODUCTION

In the past two decades, azobenzene (Az)-containing polymers, block copolymers and polymer blends or mixtures have been extensively investigated as holographic materials because of their excellent properties such as quick response, high diffraction efficiency and reversible

Address correspondence to Tomiki Ikeda, Chemical Resources Laboratory, Tokyo Institute of Technology, R1-11, 4259 Nagatsuta, Midori-ku, Yokohama, 226-8503, Japan. E-mail: tikeda@res.titech.ac.jp

storage [1–10]. Especially, the Az moieties have been attached to polymeric main chains by soft spacers to build Az-containing liquid-crystalline (LC) polymers (ALCPs), in which the Az group plays both roles as a mesogen and a photosensitive chromophore [6–14]. In the process of holographic recording in ALCP films, three kinds of contributions to the diffraction efficiency have been reported, which includes the refractive-index gratings (RIGs) induced by spatially selective photoisomerization of Az chromophores, the birefringent gratings (BGs) caused by photoinduced change in alignment of chromophores followed by that of mesogens and the surface-relief gratings (SRGs) induced by macromolecular mass transportation at the micrometer scale [6–8].

One of the most promising applications of holographic gratings is high-density information storage. To increase storage capacity, multi-processes are often explored, which has been achieved by recording SRGs on Az-containing amorphous polymers [2,5]. By adjusting optical setups for holographic recording, beat, orthogonal and other complicated structures such as Fourier-synthesized blazed grating or hexagonal-patterned SRGs have been successively obtained [2]. However, it is difficult to record complicated patterns of RIGs in ALCP films because of the molecular cooperative motion of Az mesogens in different alignment states between the bright and dark areas of the interference pattern of the writing beams. Eliminating such cooperative motion of mesogens might enable one to obtain multi-processes of RIGs. Generally, trans-Az could be an LC mesogen since the molecular shape is rod-like, whereas the cis-Az never shows any LC phase because of its bent shape [6], which has been used for the photochemical phase transition in the Az-containing LC materials or dispersed LC systems [8,16]. This gives us hints to pre-treat the ALCP films upon UV irradiation to induce a cis-Az-rich isotropic state (I) prior to holographic recording. Thus the cooperative motion of Az mesogens might be avoided, which makes is possible to record several gratings in one place of the ALCP films.

Upon irradiation of two coherent laser beams, RIGs can be recorded by selectively induced photoisomerization of Az chromophores and photochemical phase transition from an LC to an I phase in the bright areas of the interference pattern, whereas a cis-Az-rich photostationary state (an I phase) was remained in the dark areas [8,10]. Although the cis-Az can undergo thermal isomerization to the trans-Az, the LC phase cannot be easily restored under the glass-transition temperature of the ALCPs because of the high viscosity, which might enable one to obtain stable RIGs at room temperature. Furthermore, the photoresponsivity of Az molecules might be accelerated because of the lower viscosity of the pre-irradiated films in an I phase. In this paper, we report both the photoinduced alignment of Az mesogens and the multi-processes of RIGs in an ALCP film by using the pre-treatment method.

EXPERIMENTAL

Materials

As shown in Scheme 1, an ALCP with a number-average molecular weight (Mn) of 8,300 and a low polydispersity index (Mw/Mn = 1.07, measured by GPC) was synthesized by atom transfer radical polymerization (ATRP) [12]. About 20 repeat units of the Az chromophores were obtained based on the analysis of its GPC and ^{1}H NMR spectrum, and the ALCP can be expressed as PAZ20. Three kinds of phase transition peaks appeared at 69, 104 and 113°C in its thermogram by differential scanning calorimetry (DSC), corresponding to smectic X to smectic C to smectic A to I phase, respectively [12]. Two absorption peaks were observed in its UV-vis spectrum in chloroform. One stronger peak at 350 nm is due to the π-π^* transition of Az, the other peak at about 450 is attributed to n-π^* transition of Az [1].

Characterization

The PAZ20 films with a thickness of about 600 nm were prepared by spin-coating their toluene solutions on glass substrates. The thickness of the sample films was measured with a surface profiler (Veeco Instruments Inc., Dektak 3ST). Both the LC behavior and the RIG structures were examined on a polarizing optical microscope (POM,

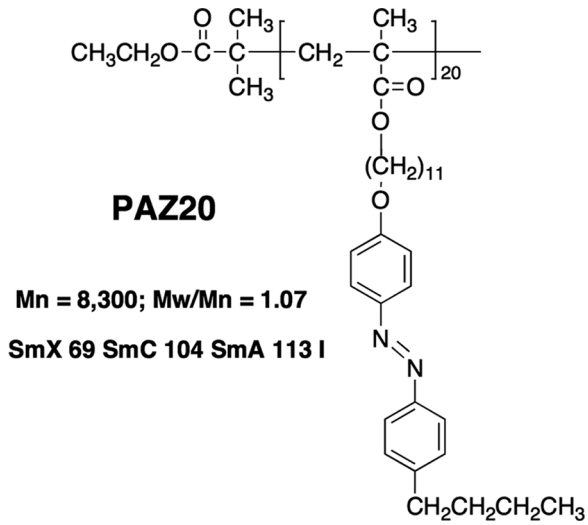

SCHEME 1 The chemical structure and properties of the azobenzene-containing liquid-crystalline polymer (PAZ20) used in this paper.

Olympus Model BH-2). Unpolarized light at 366 nm was obtained from a 500 W high-pressure mercury lamp through three glass filters (Toshiba, UV-35, UV-D36A and IRA-25). UV-vis spectra in chloroform or as a spin-coated film were measured using a JASCO U-550 spectrometer. Atomic force microscopy (AFM) images of surface modulation in tapping mode were detected with a scanning probe microscope (Veeco Instruments Inc., Nanoscope IV) at room temperature.

Photoinduced Alignment

Before photoinduced alignment, the PAZ20 films were pre-irradiated with a 366-nm unpolarized beam at an intensity of 60 mW/cm^2 for 10 min to obtain a cis-Az-rich photostationary state, in which the absorption at 488 nm was increased (Fig. 1). Then a linearly polarized beam from an Ar^+ laser (488 nm) at an intensity of 100 mW/cm^2 was used to induce the LC alignment. The optical setup for photoinduced alignment is shown in Figure 2(A). The transmittance of a He–Ne laser at 633 nm with weak intensity was monitored simultaneously during irradiation through two crossed polarizers with the sample films between them.

Holographic Recording

After pre-irradiation, the holographic gratings were recorded by a standard procedure as the optical setup shown in Figure 2(B). Two coherent laser beams with s-polarization and equal intensity of

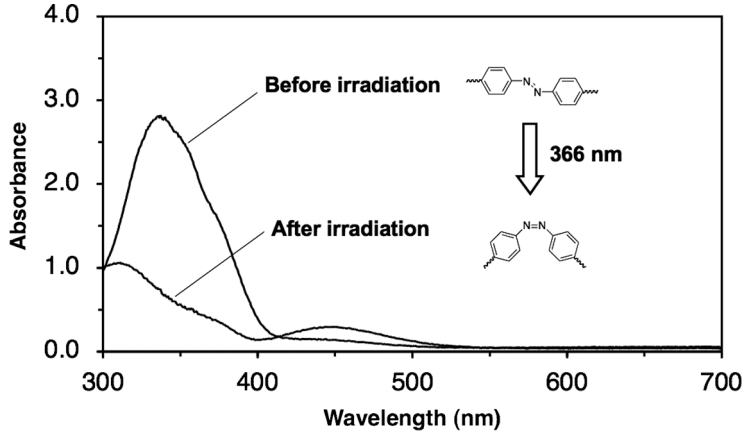

FIGURE 1 The UV-vis spectra of PAZ20 films before and after pre-irradiation at 366 nm.

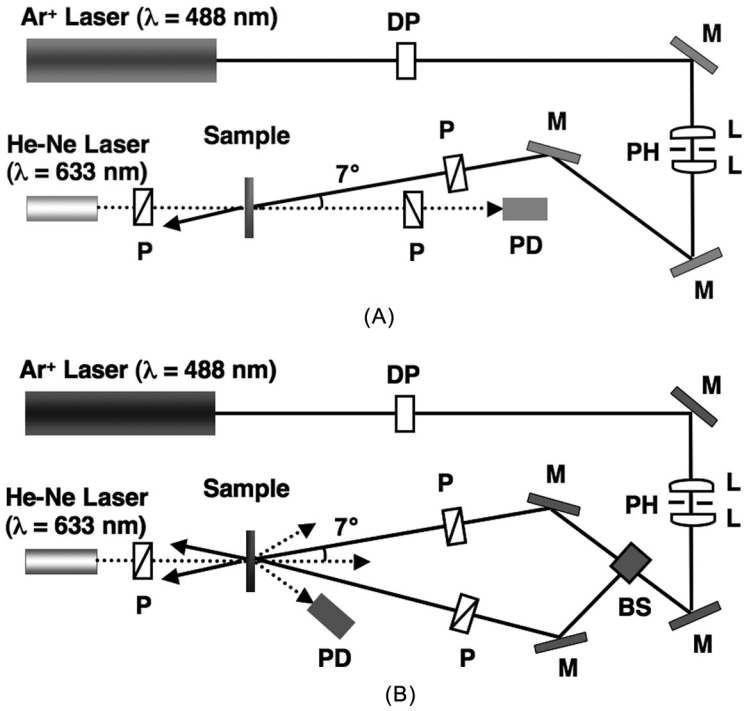

FIGURE 2 Optical setups used in this study. (A) Photoinduced LC alignment in the PAZ20 films, (B) holographic recording by interference of two coherent Ar^+ laser beams. BS, beam splitter; L, lens; M, mirror; P, polarizer; PD, photodiode; DP, depolarizer; PH, pinhole.

$50\,mW/cm^2$ from an Ar^+ laser at 488 nm were crossed on the film surface at an incident angle of 7°, leading to an interference pattern with a fringe spacing of 2.0 μm according to $\Lambda = \lambda/(2\sin\theta)$, where λ and θ are the wavelength and the incident angle of the writing laser beams, respectively. The two beams were collimated to a diameter of about 2.0 mm on the film surface. A He-Ne laser (633 nm) with weak intensity was used as a reading beam since the PAZ20 films before and after pre-irradiation have little absorption at this wavelength as shown in Figure 1. The grating formation was confirmed in real time by monitoring the intensity of the first-order diffraction beam with a photodiode in transmission mode, and the diffraction efficiency was defined as $\eta = I_1/I_0$, where I_1 is the intensity of the first-order diffraction beam, and I_0 represents the intensity of transmitted beam through the film without the writing beams, respectively. The reading beam was also normal to the film surface.

Multi-Processes of RIGs

After the first holographic grating was recorded, turning off the laser beams, then rotate the sample films by a certain degree and record the second grating by the same optical setup shown in Figure 2(B). The third grating was obtained by a similar method after rotating the sample films that have been recorded with two gratings beforehand.

RESULT AND DISCUSSIONS

It is well known that Az-containing compounds can be photoinduced alignment with their transition moments almost perpendicular to the polarization direction of the actinic beam by repeating the trans-cis-trans isomerization cycles [1,2,15]. Upon pre-irradiation, the Az alignment in the PAZ20 films was photoinduced by a linearly polarized laser beam at 488 nm. The photoinduced change in LC alignment is shown in Figure 3. On irradiation, both the isomerization of Az chromophores from cis to trans and the photochemical phase transition from an I to an LC were photoinduced, and the alignment of the Az mesogens was perpendicular to the polarization direction of the actinic beam, leading to a gradual increase in the transmittance passing through a pair of two crossed polarizers. Generally, the transmittance (T) is defined by the following equation [17],

$$T = \sin^2\left(\frac{\pi d \Delta n}{\lambda}\right)$$

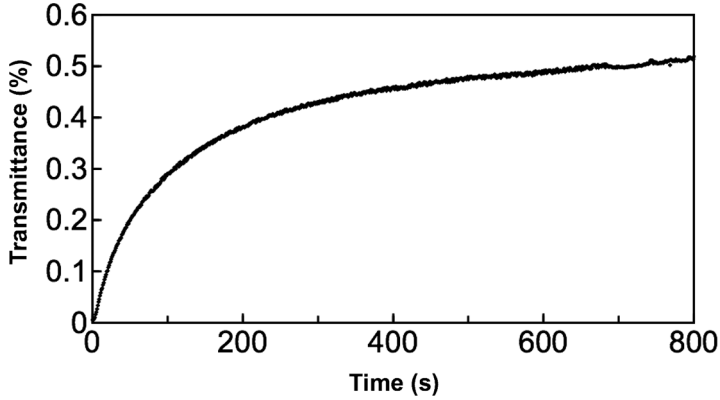

FIGURE 3 Change in transmittance of the PAZ20 films as a function of irradiation time.

where d is the film thickness, Δn is the photoinduced birefringence of the polymer film and λ is the wavelength of the probe light ($\lambda = 633$ nm). The saturated Δn of about 0.21 was obtained after irradiation for 600 s, which is larger than that of the Az-containing amorphous polymers [1].

We found that a bi-exponential function [18]

$$Y = A \times (1 - \exp(-t/t_1)) + B \times (1 - \exp(-t/t_2))$$

fits all the data in Figure 3 well, implying that at least two mechanisms are involved in the growth of photoinduced birefringence. The software of KaleidaGraph (version 3.6) was used to fit the curves and two time constants t_1 and t_2 of 16.6 and 22.5 in the equation were achieved, respectively. The obtained two parameters are smaller than those of the Az-containing amorphous polymers because of the lower velocity of the PAZ20 film in an I phase [18–20].

Three kinds of Az chromophores have been summarized by Natansohn and Kumar [1,15]. The first "Az" has relatively poor π-π^* and n-π^* absorbance overlap and the lifetime of the cis-isomer is relatively long. The second one is "aminoazobenzenes", and there is significant overlap of the two bands and the cis-isomer lifetime is shorter. The third Az is "pseudostilbenes", where the Az is usually substituted with electron-donor and electron-acceptor substituents. Considering the molecular structure and photoresponsive behavior, the Az in the present PAZ20 belongs to the first kind.

Such kind of ALCPs showed little surface relief if no low-molecular-weight LC (e.g., 5CB) was mixed [16]. As show in Figure 4(A), a surface relief of about 3 nm with a grating periodicity of 2.0 μm was obtained after recording for 2 s. No obvious increase in the surface relief was observed with a longer irradiation time. In this study, all experiments were performed in the Raman-Nath regime (thin film), and multiple diffraction beams were observed.

Although little formation of the surface relief was induced on the sample films, the RIG structures with the same grating periodicity of 2.0 μm as that of the SRG were clearly observed by POM as shown in Figure 4(B). The bright areas of the interference pattern correspond to the bright stripes of the POM images (LC phase), whereas the dark areas are correlated with dark stripes of the POM images (I phase), which is contrary to our previous results of ALCPs since pre-irradiation was carried out beforehand [7]. The RIG structures were stable under room light because of the long lifetime of the cis-Az in PAZ20 films. No detectable change in POM pictures was observed after being stored at room temperature for two months.

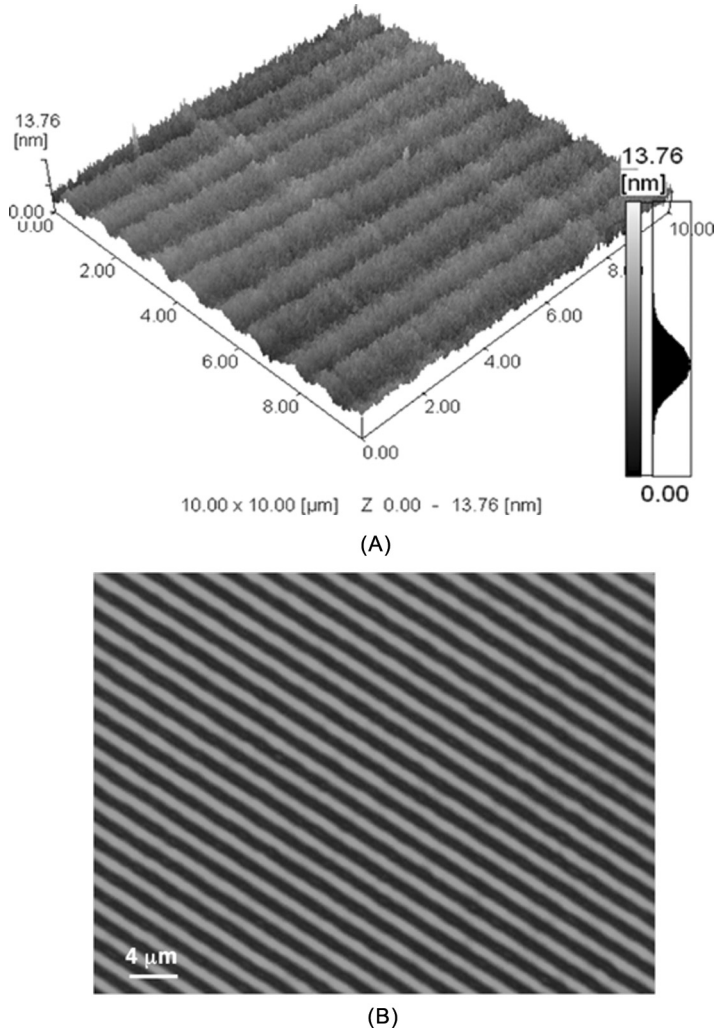

FIGURE 4 AFM topological image (A) and polarizing optical micrograph (B) of the holographic gratings recorded in the PAZ20 film.

Since the surface relief of the grating is very small, the contribution of the SRG to the diffraction efficiency (η) can be omitted. Based on the special modulation of the refractive index, η can be calculated theoretically by the following equation,

$$\eta = \left(\frac{\pi d \Delta n'}{\lambda}\right)^2$$

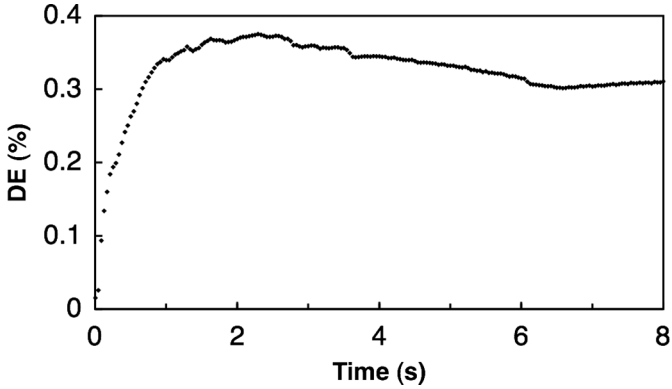

FIGURE 5 Evolution of the first-order diffraction efficiency of holographic gratings recorded in the pre-treated PAZ20 films as a function of recording time.

Where d and λ are film thickness and the wavelength of the reading beam, respectively. $\Delta n'$ is the difference in the refractive index between the bright (an LC phase) and dark (an I phase) fringes. As shown in Figure 5, the maximum η of 0.38% was obtained after holographic recording for 2 s, leading to the $\Delta n'$ of 0.021.

To record the second gratings and investigate the corresponding structure of the RIGs, the grating sample obtained with the maximum η at 2 s was rotated by 90°. Using the same the optical setups shown in Figure 2(B) to record the second grating for another 2 s. Two processes of the RIGs were successfully obtained as shown in Figure 6(A). The perpendicular RIG structures clearly observed under POM were also indicated by the image of the first-order diffraction beams of the RIGs. The patterning width of the second orthogonal grating was also 2.0 μm, the same as that of the grating by one process. Then three processes of the RIGs were obtained by the similar method. As shown in Figure 6(B), the POM picture shows an angle of 60° between two gratings, correlating with the position of sample films shown in the left of the Figures. The diffraction picture is given in the right side of the POM image.

CONCLUSION

We studied the photoinduced LC alignment in an ALCP film after being pre-irradiated by unpolarized UV light. A large birefringence of 0.21 was obtained by one linearly polarized laser beam. Upon irradiation of interference of two coherent laser beams, holographic gratings were recorded

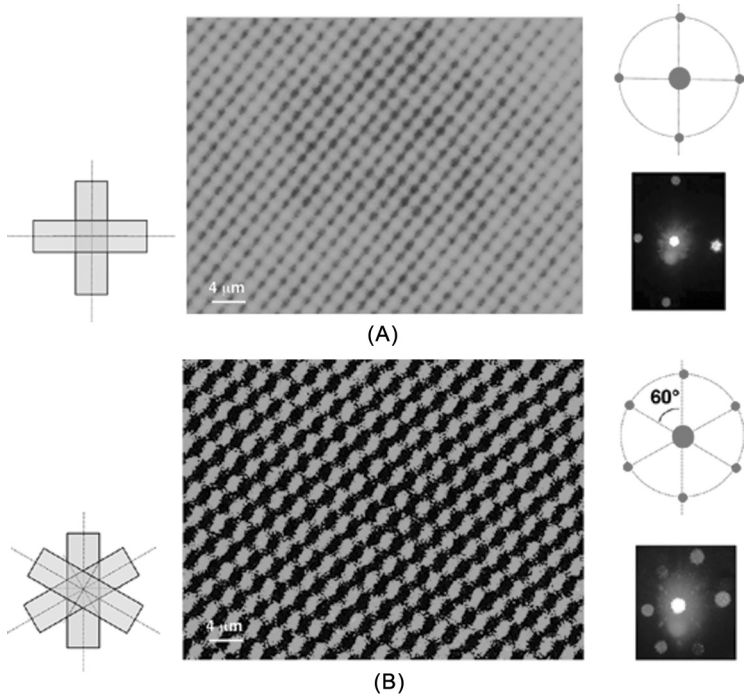

FIGURE 6 Polarizing optical micrographs of multi-processes of the RIGs, (A) two processes (B) three processes. The left and right sides of every micrograph are the scheme of the sample positions and the pictures of first-order diffraction beams, respectively.

in the pre-treated films. The RIG paid most of contributions to the diffraction efficiency because little surface relief was obtained. By the pre-treatment method, the cooperative motion of Az mesogens in PAZ20 films were eliminated, and multi-processes of the RIGs were successively obtained, indicating that the Az-containing polymer has potential application in high-density information storage.

REFERENCES

[1] Natansohn, A. & Rochon, P. (2002). *Chem. Rev.*, *102*, 4139.
[2] Viswanathan, N., Kim, D., Bian, S., Williams, J., Liu, W., Li, L., Samuelson, L., Kumar, J., & Tripathy, S. (1999). *J. Mater. Chem.*, *9*, 1941.
[3] Todorov, T., Nikolova, L., & Tomova, N. (1984). *Appl. Optics.*, *23*, 4309.
[4] Rochon, P., Batalla, E., & Natanhson, A. (1995). *Appl. Phys. Lett.*, *66*, 136.
[5] Kim, D. Y., Tripathy, S. K., Li, L., & Kumar, J. (1995). *Appl. Phys. Lett.*, *66*, 1166.

[6] Ikeda, T. (2003). *J. Mater. Chem.*, *13*, 2037.
[7] Yamamoto, T., Hasagawa, M., Kanazawa, A., Shiono, T., & Ikeda, T. (1999). *J. Phys. Chem. B*, *103*, 9873.
[8] Yu, H. F., Okano, K., Shishido, A., Ikeda, T., Kamata, K., Komura, M., & Iyoda, T. (2005). *Adv. Mater.*,*17*, 2184.
[9] Yu, H. F., Shishido, A., Ikeda, T., & Iyoda, T. (2005). *Macromol. Rapid Commun.*, *26*, 1594.
[10] Yu, H. F., Iyoda, T., Okano, K., Shishido, A., & Ikeda, T. (2005). *Mol. Cryst. Liq. Cryst.*, *443*, 191.
[11] Ikeda, T. & Tsutsumi, O. (1995). *Science*, *268*, 1873.
[12] Tian, Y. Q., Watanabe, K., Kong, X. X., Abe, J., & Iyoda, T. (2002). *Macromolecules*, *35*, 3739.
[13] Yu, H. F., Iyoda, T., & Ikeda, T. (2006). *J. Am. Chem. Soc.*, *128*, 11010.
[14] Yu, H. F., Li, J. Z., Iyoda, T., & Ikeda, T. (2006). *Adv. Mater.*, *18*, 2213.
[15] Kumar, G. S. & Neckers, D. C. (1989). *Chem. Rev.*, *89*, 1915.
[16] Seki, T. (2004). *Polym. J.*, *36*, 435.
[17] Crossland, W. A. & Wilkinson, T. D. (1998). In: *Handbook of Liquid Crystals*, Demus, D., Goodby, J., Gray, G. W., Spiess, H.-W., & Vill, V. (Eds.), Wiley-VCH: Weinheim, Germany, Vol. 1, 771.
[18] Ho, M. S., Natansohn, A., & Rochon, P. (1995). *Macromolecules*, *28*, 6124.
[19] Cha, S. W., Choi, D. H., & Jin, J. I. (2001). *Adv. Funct. Mater.*, *11*, 355.
[20] Cha, S. W., Choi, D. H., Oh, D. K., Han, D. Y., Lee, C. E., & Jin, J. I. (2002). *Adv. Funct. Mater.*, *12*, 670.